Summary of the 2013/2014 Asian Winter Monsoon

This report summarizes the characteristics of the surface climate and atmospheric/oceanographic considerations related to the Asian winter monsoon for 2013/2014.

Note: Japanese 55-year Reanalysis (JRA-55; http://jra.kishou.go.jp/JRA-55/index_en.html) atmospheric circulation data and COBE-SST (JMA 2006) sea surface temperature (SST) data were used for this investigation. The outgoing longwave radiation (OLR) data referenced to infer tropical convective activity were originally provided by NOAA. The base period for the normal is 1981 – 2010. The term "anomaly" as used in this report refers to deviation from the normal.

1. Surface climate conditions

1.1 Overview of Asia

In boreal winter 2013/2014, temperatures were above or near normal in many parts of East Asia and in eastern Siberia, and were below normal in many parts of South, Southeast and Central Asia (Figure 9). Very high or low temperatures were recorded on a regional scale in December, January and February, but were not seen on this scale in the three-month mean field.

Figure 10 shows extreme climate events observed from December 2013 to February 2014. In December, extremely high temperatures were observed in Mongolia and Siberia, and extremely low temperatures were recorded on the Indochina Peninsula and in southern China. Extremely heavy precipitation amounts were observed over parts of Southeast Asia. In January, extremely high temperatures were seen in Mongolia and in northern and eastern China, while extremely low temperatures were seen around the South China Sea. In February, extremely low temperatures were observed in Central Asia and the eastern Middle East. Extremely heavy precipitation amounts were observed in parts of Japan, and extremely light precipitation amounts were seen in parts of Indonesia and on the Malay Peninsula.

Figure 11 shows time-series representations of daily temperatures at Bangkok in Thailand and Astana in Kazakhstan for winter 2013/2014. Daily mean temperatures were below normal in the second halves of December and January and near normal for other parts of winter at Bangkok. Daily mean temperatures were above normal on many days in December and below normal on most days from the second half of January to the end of February at Astana.

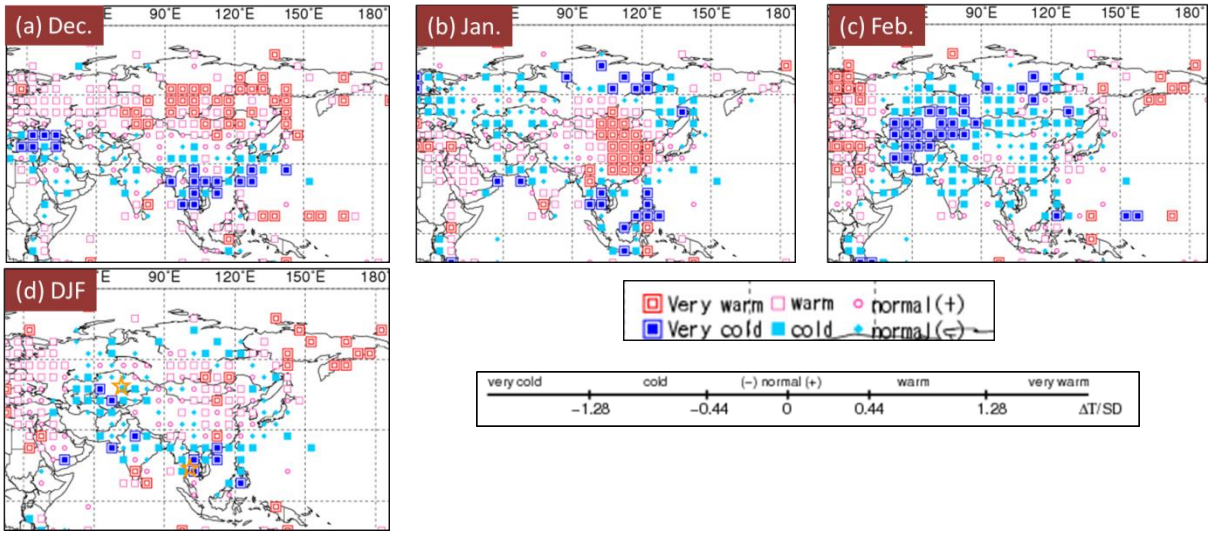

Figure 9 Monthly mean temperature anomalies for (a) December 2013, (b) January 2014 and (c) February 2014, and (d) three-month mean temperature anomalies for December 2013 – February 2014

Categories are defined by the monthly/three-month mean temperature anomaly against the normal divided by its standard deviation and averaged in 5° × 5° grid boxes. The thresholds of each category are -1.28, -0.44, 0, +0.44 and +1.28. Standard deviations were calculated from 1981 – 2010 statistics. Areas over land without graphical marks are those where observation data are insufficient or where normal data are unavailable. In (d), the orange stars indicate the locations of Bangkok (Thailand) and Astana (Kazakhstan). Daily temperature data for both cities are shown in Figure 11.

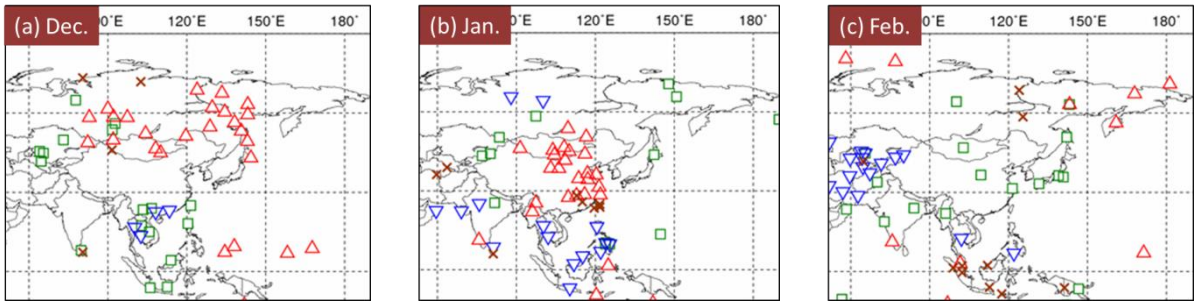

Figure 10 Extreme climate events for (a) December 2013, (b) January 2014 and (c) February 2014

△ Extremely high temperature (ΔT/SD > 1.83) □ Extremely heavy precipitation (Rd = 6)

▽ Extremely low temperature (ΔT/SD < -1.83) × Extremely light precipitation (Rd = 0)

ΔT, SD and Rd indicate temperature anomaly, standard deviation and quintile, respectively.

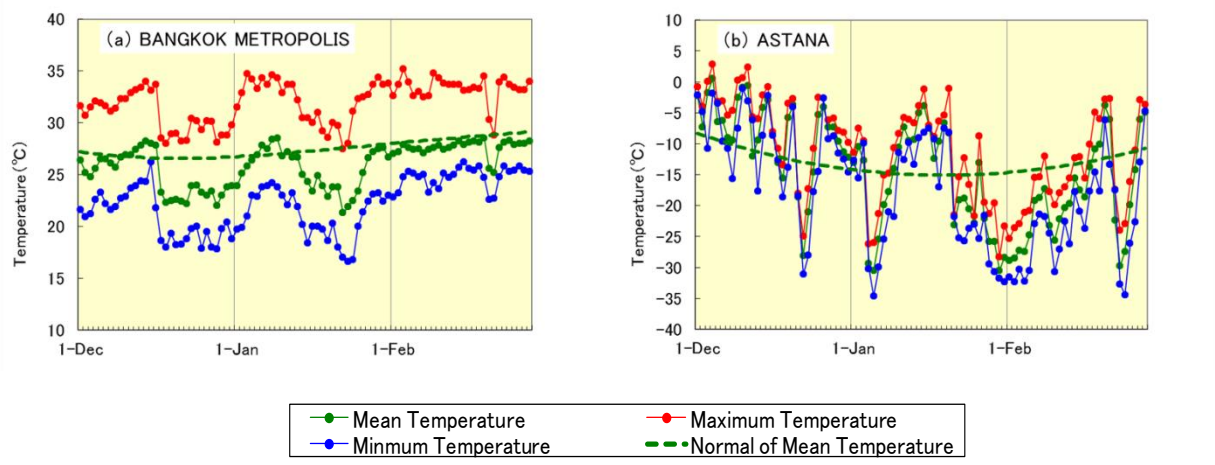

Figure 11 Time-series representation of daily maximum, mean and minimum temperatures (°C) at Bangkok in Thailand and Astana in Kazakhstan from 1 December 2013 to 28 February 2014 (based on SYNOP reports)

1.2 Heavy snowfall over northern and eastern Japan in February 2014

The Pacific side of northern and eastern Japan experienced two heavy snowfall events in February 2014. The one that occurred in mid-February had a devastating impact on socio-economic activities.

A developing low-pressure system forming on 13 February moved northeastward to the south of mainland Japan and reached the eastern part of northern Japan on 16 February. In association with this system, snow fell over a wide area mainly on the Pacific side from western to northern Japan. Some parts of the north's Tohoku region and the east's Kanto/Koshin region experienced record-breaking snowfall from 14 to 15 February. Northern Japan was also hit by heavy snowfall and severe snowstorms from 15 to 19 February.

New records for maximum snow depth were set at 18 stations in northern Japan and in the Kanto/Koshin region (for stations with statistics spanning a period of over 10 years) (Table 1 and Figure 12). In Tokyo, the maximum snow depth of 27 cm was the joint eighth highest since 1875. According to the Cabinet Office, the event in mid-February claimed 26 lives across the country and had a heavy socio-economic impact.

Table 1 Selected stations observing record snow depths on 15 February 2014

Station Name (Prefecture)	Maximum snow depth	Previous record (year)	Data Since
Shirakawa (Fukushima)	76 cm	74 cm (1946)	1940
Utsunomiya (Tochigi)	32 cm	30 cm (1945)	1890
Maebashi (Gunma)	73 cm	37 cm (1945)	1896
Kumagaya (Saitama)	62 cm	45 cm (1936)	1896
Kofu (Yamanashi)	114 cm	49 cm (1998)	1894
Karuizawa (Nagano)	99 cm	72 cm (1998)	1925

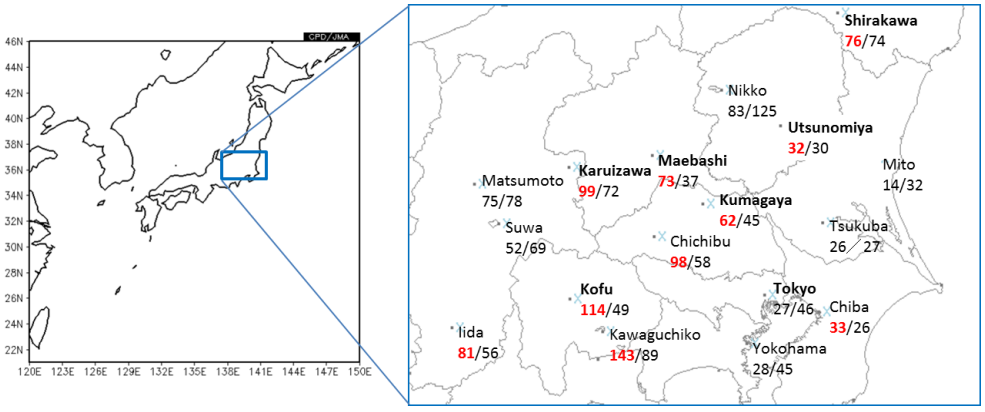

Figure 12 Maximum snow depths (cm) at selected stations in the Kanto/Koshin region

The values on the left and right indicate maximum snow depths recorded on 15 February 2014 (except Chiba, Tsukuba and Mito, whose data are from 9 February) and record-high snow depths, respectively. Values in red denote new records.

2. Characteristic atmospheric circulation and oceanographic conditions

2.1 Overview of the tropics and Southeast Asia

In winter 2013/2014, sea surface temperatures (SSTs) were above normal in the western equatorial Pacific and below normal in the central and eastern equatorial Pacific (Figure 13). SST anomalies indicated warm conditions in the South Indian Ocean and cold conditions in the North Indian Ocean and the South China Sea. Active convection areas compared to the normal gradually moved eastward from the Indian Ocean in December to the dateline region in February (Figure 14 (b)). In the western equatorial Pacific, significant westerly wind anomalies (westerly wind burst events) were seen in the second half of January and the period from the second half of February to early March (Figure 14 (c)). This activity during the latter period was associated with the Madden-Julian Oscillation (Figure 14 (a)).

In December 2013, large-scale divergence anomalies in the upper troposphere over the Indian Ocean and the Maritime Continent (Figure 15 (a)) indicated enhanced convective activity that contributed to heavy rainfall over parts of the Maritime Continent. Upper-level large-scale convergence anomalies were seen over the dateline region, indicating suppressed convective activity there. In the 850-hPa stream function field, cyclonic and anti-cyclonic circulation anomalies straddling the equator were observed over the Indian Ocean and the western Pacific, respectively (Figure 16 (a)), in association with the anomalous convective activity seen over the Indian Ocean and the Pacific.

In January 2014, large-scale divergence anomalies in the upper troposphere were seen over the eastern Maritime Continent and the western Pacific (Figure 15 (b)). In the lower troposphere, a pair of cyclonic circulation anomalies was centered near the Philippines and the northern coast of Australia, with northerly wind anomalies around the South China Sea and strong westerly wind anomalies over the western equatorial Pacific (Figure 16 (b)). The results of linear baroclinic model experiments forced with convective heating and cooling anomalies over the tropics show such lower-level circulation anomaly patterns and below-normal temperatures around the South China Sea (Figure 17). It can therefore be presumed that anomalous convective activity in the tropics contributed to stronger-than-normal northerly winds and extremely low temperatures over the Indochina Peninsula and the Philippines.

In February 2014, large-scale divergence anomalies in the upper troposphere were seen over the western Pacific and the dateline region, and convergence anomalies were observed over the Maritime Continent (Figure 15 (c)), contributing to dry conditions in parts of Indonesia and on the Malay Peninsula. In the lower troposphere, a pair of cyclonic circulation anomalies was seen over the western Pacific with strong westerly wind anomalies over its equatorial area (Figure 17). Such anomaly patterns were displaced eastward of those observed in January.

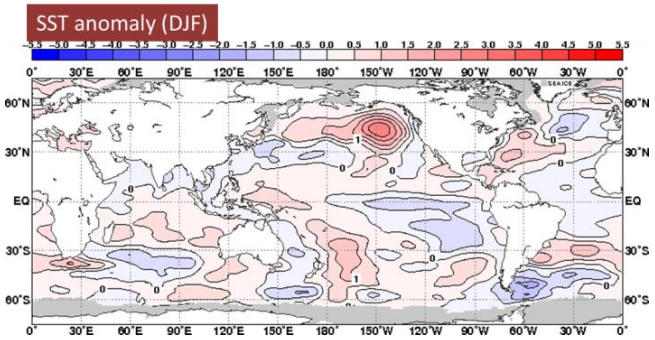

Figure 13 Three-month mean sea surface temperature (SST) anomalies for December 2013 – February 2014

The contour interval is 0.5˚C.

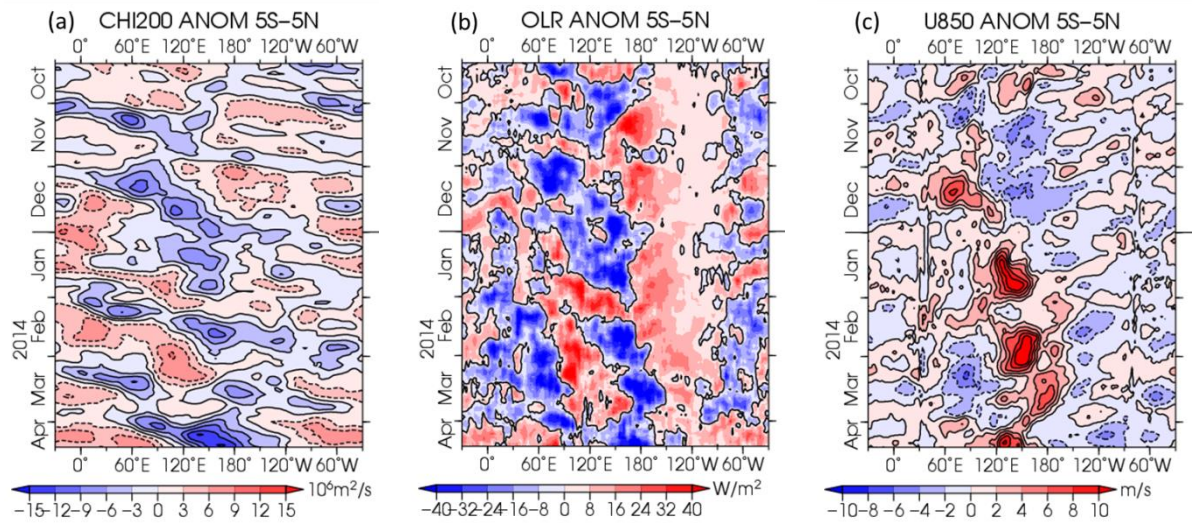

Figure 14 Time-longitude cross section of seven-day running mean (a) 200-hPa velocity potential anomalies, (b) outgoing longwave radiation (OLR) anomalies, and (c) 850-hPa zonal wind anomalies around the equator (5°S – 5°N) from mid-October 2013 to mid-April 2014

(a) The contour interval is 3×10^6 m^2/s. The blue and red shading indicates areas of divergence and convergence anomalies, respectively. (b) The blue and red shading indicates areas of enhanced and suppressed convective activity, respectively. (c) The contour interval is 2 m/s. The blue and red shading shows easterly and westerly wind anomalies, respectively.

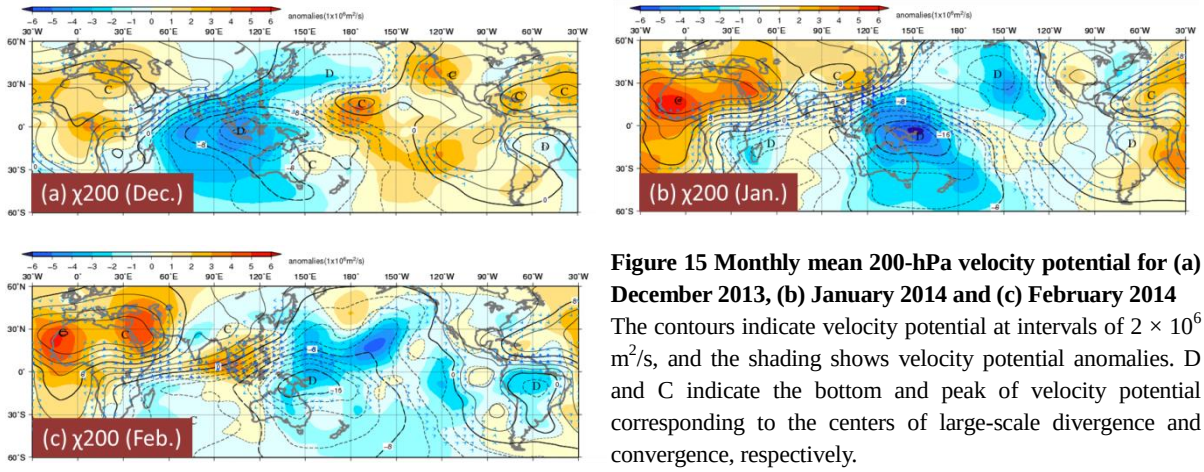

Figure 15 Monthly mean 200-hPa velocity potential for (a) December 2013, (b) January 2014 and (c) February 2014

The contours indicate velocity potential at intervals of 2×10^6 m^2/s, and the shading shows velocity potential anomalies. D and C indicate the bottom and peak of velocity potential corresponding to the centers of large-scale divergence and convergence, respectively.

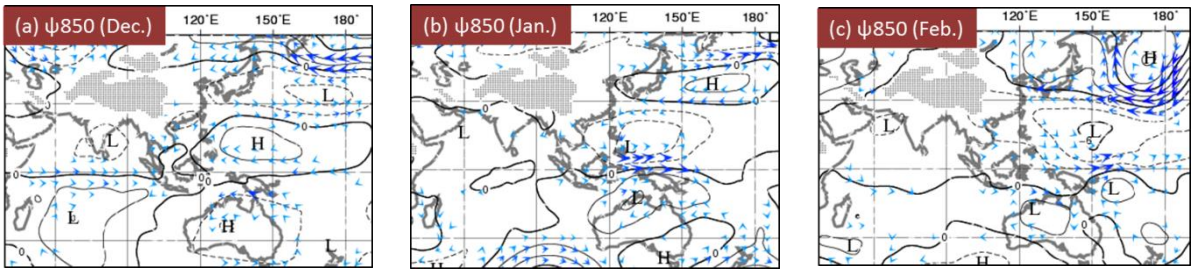

Figure 16 Monthly mean 850-hPa stream function anomalies and wind vector anomalies for (a) December 2013, (b) January 2014 and (c) February 2014

The contours indicate stream function anomalies at intervals of 2×10^6 m^2/s, and vectors show wind vector anomalies. H and L indicate the centers of anticyclonic and cyclonic circulation anomalies, respectively.

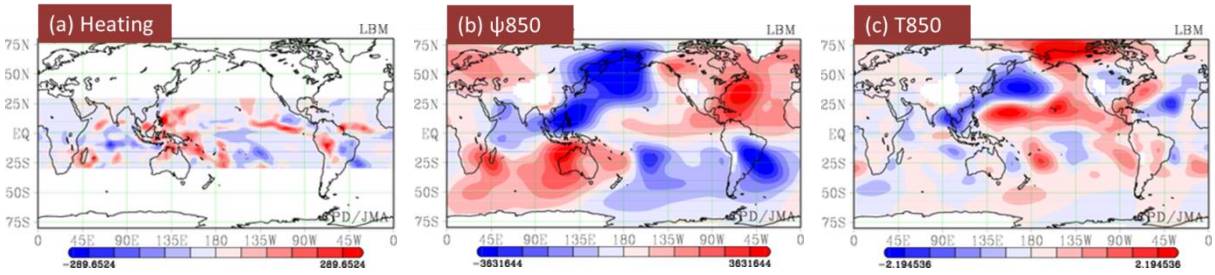

Figure 17 Steady response to heating anomalies in the tropics for January 2014 in a linear baroclinic model (LBM)

(a) The red and blue shading indicates diabatic heating and cooling, respectively, for the LBM with the basic state for January (i.e., the 1981 – 2010 average). (b) The shading denotes the steady response of 850-hPa stream function anomalies (m^2/s). (c) The shading shows the steady response of 850-hPa temperature anomalies (°C). These anomalies as responses represent deviations from the basic states, and are additionally subtracted from the zonal averages of the anomalies.

2.2 Overview of the Northern Hemisphere and East Asia

In winter 2013/2014, the polar vortex tended to be shifted toward Canada in the 500-hPa height field, and distinct troughs persisted over the central-eastern part of North America (Figure 18). In association, Arctic cold air frequently flowed over a large area of North America and caused cold conditions there, especially over the Midwest area of the USA (Figure 19). Strong low-pressure systems centered to the northwest of the UK persisted during the winter (Figure 20), contributing to significantly above-normal rainfall in the country. The intensity of the Siberian High varied significantly with a period of approximately 30 days (Figure 21 (a)), and its winter average showed normal intensity (Figure 21 (b)).

In December 2013, blocking ridges were seen over Siberia (Figure 18 (a)), contributing to extremely warm conditions there (Figure 10 (a)). In January 2014, the polar vortex was split into two in association with the development of ridges seen over the Arctic Ocean, and one of the two vortices with Arctic cold air was displaced over Siberia (Figure 18 (b)), contributing to below-normal temperatures in the region (Figure 9 (b)). Zonally elongated positive anomalies were seen over East Asia, indicating that the polar-front jet stream exhibited no tendency to meander southward over the region compared to the normal. In association, China and Mongolia experienced extremely warm conditions (Figure 10 (b)). In February 2014, the polar vortex was split into two and displaced toward Canada and central Siberia, and blocking ridges developed over eastern Siberia and northwestern Russia (Figure 18 (c)). In association, temperatures were above normal in eastern Siberia and below normal in its western and central parts (Figure 19 (c)).

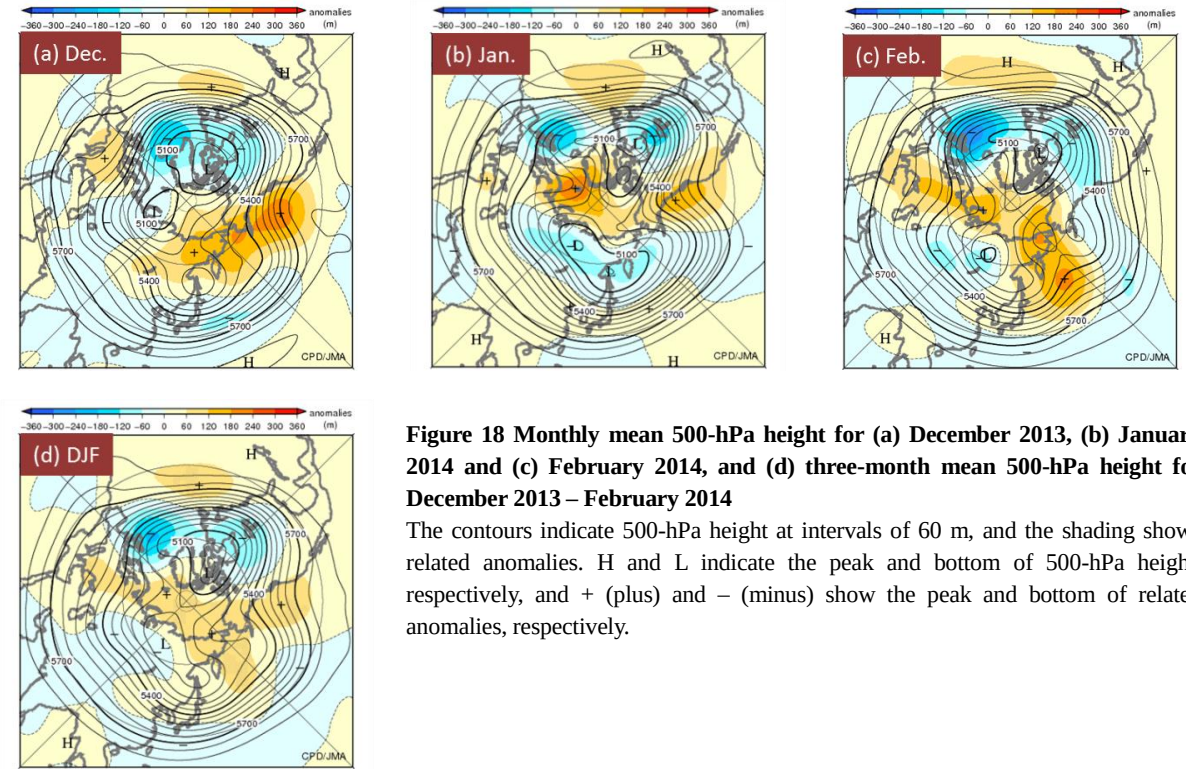

Figure 18 Monthly mean 500-hPa height for (a) December 2013, (b) January 2014 and (c) February 2014, and (d) three-month mean 500-hPa height for December 2013 – February 2014

The contours indicate 500-hPa height at intervals of 60 m, and the shading shows related anomalies. H and L indicate the peak and bottom of 500-hPa height, respectively, and + (plus) and – (minus) show the peak and bottom of related anomalies, respectively.

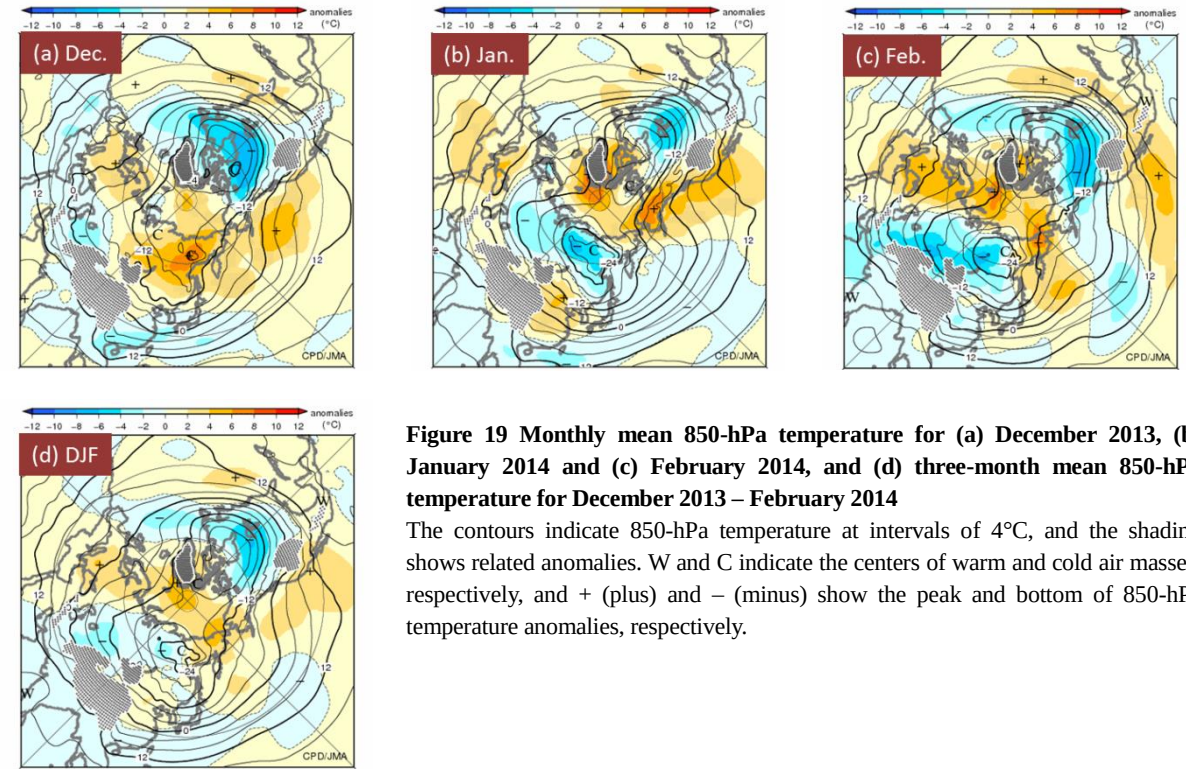

Figure 19 Monthly mean 850-hPa temperature for (a) December 2013, (b) January 2014 and (c) February 2014, and (d) three-month mean 850-hPa temperature for December 2013 – February 2014

The contours indicate 850-hPa temperature at intervals of 4°C, and the shading shows related anomalies. W and C indicate the centers of warm and cold air masses, respectively, and + (plus) and – (minus) show the peak and bottom of 850-hPa temperature anomalies, respectively.

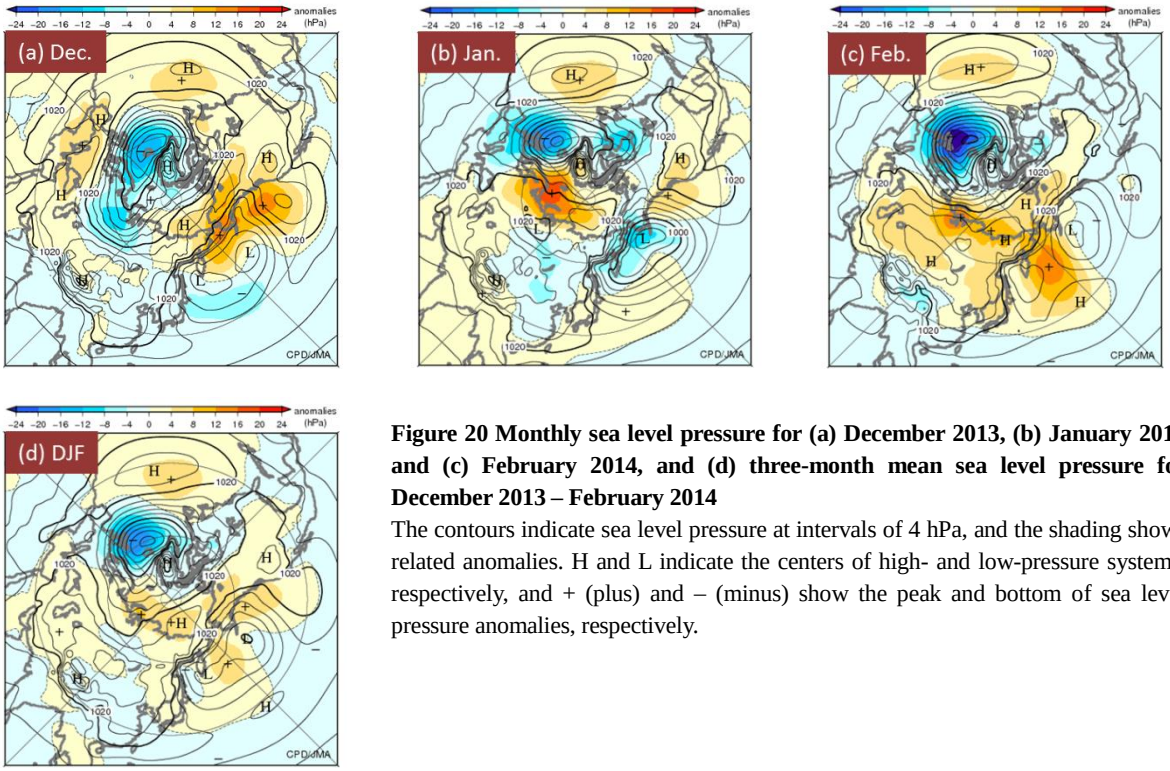

Figure 20 Monthly sea level pressure for (a) December 2013, (b) January 2014 and (c) February 2014, and (d) three-month mean sea level pressure for December 2013 – February 2014

The contours indicate sea level pressure at intervals of 4 hPa, and the shading shows related anomalies. H and L indicate the centers of high- and low-pressure systems, respectively, and + (plus) and – (minus) show the peak and bottom of sea level pressure anomalies, respectively.

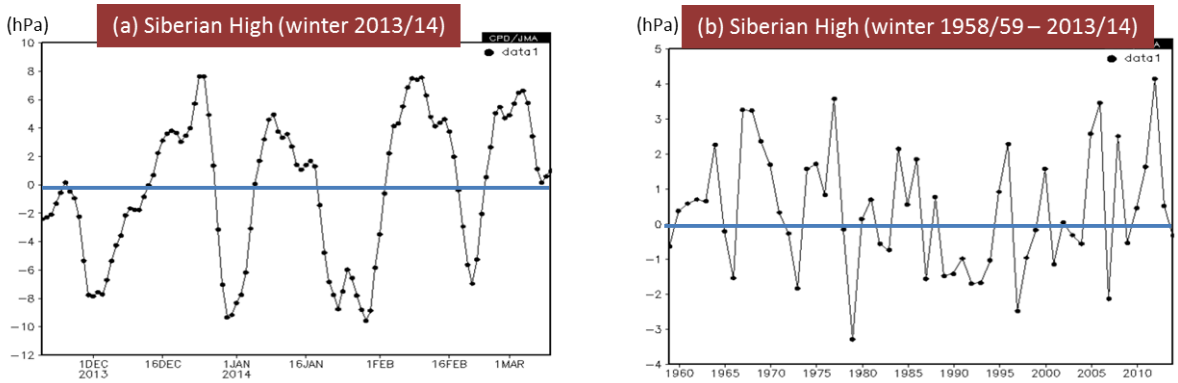

Figure 21 (a) Intraseasonal and (b) interannual variations of area-averaged sea level pressure anomalies around the center of the Siberian High (40°N – 60°N, 80°E – 120°E) for winter

(a) The black line indicates five-day running mean values for the period from 20 November 2013 to 10 March 2014. (b) The black line indicates three-month mean values for December-January-February from 1958/1959 to 2013/2014.

3. Summary

Extreme climate events were seen for relatively short periods in parts of Asia in winter 2013/2014, but none persisted widely.

References

Ebita, A., S. Kobayashi, Y. Ota, M. Moriya, R. Kumabe, K. Onogi, Y. Harada, S. Yasui, K. Miyaoka, K. Takahashi, H. Kamahori, C. Kobayashi, H. Endo, M. Soma, Y. Oikawa, and T. Ishimizu, 2011: The Japanese 55-year Reanalysis "JRA-55": an interim report, SOLA, 7, 149-152.

JMA, 2006: Characteristics of Global Sea Surface Temperature Data (COBE-SST), *Monthly Report on Climate System*, Separated Volume No. **12**.